Syst. Biol. 65(3):417–431, 2016
© The Author(s) 2016. Published by Oxford University Press, on behalf of the Society of Systematic Biologists. All rights reserved.
For Permissions, please email: journals.permissions@oup.com
DOI:10.1093/sysbio/syw010
Advance Access publication February 23, 2016

Bridging Inter- and Intraspecific Trait Evolution with a Hierarchical Bayesian Approach

Anna Kostikova[1,2], Daniele Silvestro[1,2,3], Peter B. Pearman[4,5], and Nicolas Salamin[1,2,*]

[1]*Department of Ecology and Evolution, University of Lausanne, 1015 Lausanne, Switzerland;* [2]*Swiss Institute of Bioinformatics, Quartier Sorge, 1015 Lausanne, Switzerland;* [3]*Department of Biological and Environmental Sciences, University of Gothenburg, Carl Skottsbergsgata 22B, 413 19 Gothenburg, Sweden;* [4]*Department of Plant Biology and Ecology, University of the Basque Country UPV/EHU, 48940 Leioa, Spain; and* [5]*IKERBASQUE, Basque Foundation for Science, 48013 Bilbao, Spain.*
**Correspondence to be sent to: Biophore, 1015 Lausanne, Switzerland; Email: nicolas.salamin@unil.ch*

Anna Kostikova and Daniele Silvestro contributed equally to this article.

Received 26 March 2014; reviews returned 4 January 2016; accepted 11 January 2016
Associate Editor: Luke Harmon

Abstract.—The evolution of organisms is crucially dependent on the evolution of intraspecific variation. Its interactions with selective agents in the biotic and abiotic environments underlie many processes, such as intraspecific competition, resource partitioning and, eventually, species formation. Nevertheless, comparative models of trait evolution neither allow explicit testing of hypotheses related to the evolution of intraspecific variation nor do they simultaneously estimate rates of trait evolution by accounting for both trait mean and variance. Here, we present a model of phenotypic trait evolution using a hierarchical Bayesian approach that simultaneously incorporates interspecific and intraspecific variation. We assume that species-specific trait means evolve under a simple Brownian motion process, whereas species-specific trait variances are modeled with Brownian or Ornstein–Uhlenbeck processes. After evaluating the power of the method through simulations, we examine whether life-history traits impact evolution of intraspecific variation in the Eriogonoideae (buckwheat family, Polygonaceae). Our model is readily extendible to more complex scenarios of the evolution of inter- and intraspecific variation and presents a step toward more comprehensive comparative models for macroevolutionary studies. [Comparative phylogenetics; hierarchical Bayesian model; intraspecific variance; macroevolution; Markov Chain Monte Carlo; niche breadth.]

Over the past decade, comparative methods have become a standard tool for most macroevolutionary analyses (O'Meara 2012). The increased interest in these analyses has also fostered tremendous development of models for studying the evolution of species phenotypes. In turn, these methodological advances have expanded the types of analyses that can be performed on phylogenetic data, allowing comparison of a wide range of alternative hypotheses describing the evolutionary history of species (Felsenstein 1985; Hansen 1997a; Butler and King 2004; O'Meara et al. 2006; Beaulieu et al. 2012). Most of these developments have targeted the evolution of species mean phenotypes, whereas the treatment of intraspecific variability has received less attention. Differences in within-species measurements come from two sources: (1) heterogeneity in sampling effort and measurement error and (2) true differences between populations or individuals (Garamszegi and Møller 2010; Hansen and Bartoszek 2012). In addition to developments on the modeling of mean phenotypes, much progress has been made to incorporate measurement error into comparative models and it is now possible to account for sampling errors through Bayesian methods (Revell and Reynolds 2012), bias-corrected estimators in linear models (Hansen and Bartoszek 2012), and mixed models (Lynch 1991; Ives et al. 2007; Felsenstein 2008). These methods provide a way to incorporate population-level measurements into the models, but the integration of individual data is not yet fully applicable (Felsenstein 2008). Furthermore, while these methods considerably improve the accuracy of estimated mean phenotypes and remove potential biases in model comparison (Silvestro et al. 2015), explicit modeling of the evolution of true intraspecific variability has been largely overlooked (Salamin et al. 2010). This is problematic because within-species variation almost certainly exists in any given species (Garamszegi and Møller 2010) and enables species evolution and diversification (Darwin 1859; MacArthur 1965). Alternatively, the quantitative genetic theory and more specifically the theory of mutation-selection balance could also provide a substantive ground to characterize the evolution of intraspecific variation. It is, however, difficult to explicitly translate these theories to the species-level processes that are modeled in macroevolution (Hansen and Houle 2008; Hansen and Bartoszek 2012; Bolstad et al. 2014).

The response of intraspecific variation to the environment is crucial for many processes operating at macro- and microevolutionary scales (MacArthur and Levins 1964; Roughgarden 1972; Whitlock 1996; Bolnick 2001; Kassen 2002; Ackermann and Doebeli 2004). For instance, cryptic speciation of phylogenetically young clades depends on the genetic and phenotypic intraspecific variation present in a population (Grant and Price 1981; Evans et al. 2009). Intraspecific variation also plays an important role in the process of interspecific competition (MacArthur 1965), influences community composition (Violle et al. 2012), and underlies the rapid adaptation of species to novel environments (Urbanski et al. 2012). Furthermore, both comparative and experimental evidence suggests that intraspecific variation itself can readily respond to selection (Nosil

Downloaded from https://academic.oup.com/sysbio/article-abstract/65/3/417/2468958 by UB Leipzig user on 25 October 2019

2002; Ackermann and Doebeli 2004; Bolnick et al. 2011). For example, within-species variation in floral traits increases in response to antagonistic interactions and decreases in response to mutualistic plant–pollinator interactions (Herrera 1996). Similarly, life-history traits and changes in environmental predictability along elevational gradients drive the evolution of wider climatic niche breadth (generalization) in North American eriogonoids (Kostikova et al. 2013). Nevertheless, explicit macroevolutionary models of intraspecific evolution are difficult to construct. Contrary to models that consider the evolution of phenotypic means, the theories on intraspecific variation that can be derived from quantitative genetics models of microevolutionary change (Lande 1976; Turelli et al. 1988; Hansen and Martins 1996) are difficult to extrapolate to larger evolutionary scales (Hansen and Martins 1996; Hansen 1997a; Martins and Hansen 1997). A notable exception is when intraspecific variation is considered as measurement artifact (Lynch 1991; Ives et al. 2007; Felsenstein 2008).

In contrast, some ecological geneticists regard intraspecific variance as a heritable trait, although some of these theories are still lacking firm empirical evidence (Schluter 2000). For example, using this notion of intraspecific variation, Roughgarden (1972) shows that ecological release increases the intraspecific variation of sexual populations. Similarly, Ackermann and Doebeli (2004) investigate the necessary circumstances for competition among conspecifics to result in decreased intraspecific variation and adaptive divergence of lineages. Specifically, Ackermann and Doebeli (2004) identify that for a broadly distributed resource, adaptive diversification is likely when niche breadth (Hutchinson 1978) is fixed and narrow (there is a cost to niche generalization), but niche optimum is free to evolve. Furthermore, life-history traits are known to affect the evolution of specialist species (little intraspecific variation) and generalist species (substantial intraspecific variation) in both experimental (Kassen 2002) and theoretical studies (Whitlock 1996). If we assume that intraspecific variation behaves as a heritable trait in a manner similar to phenotypic means, then the evolution of such variation can also be traced along the branches of a phylogenetic tree. This will require extension of existing models to include within-species variation and modeling it together with the evolution of the phenotypic means. Moreover, these two stochastic processes can be decoupled in the modeling framework, because there are well-developed reasons to assume that the evolution of species mean phenotype and phenotypic variance are potentially independent (Roughgarden 1983).

This study presents a model of Joint Inter- and intraspecific Variance Evolution (the JIVE model) integrated into a hierarchical Bayesian framework. The approach simultaneously estimates the evolution of phenotypic means, variances, and the parameters of the underlying evolutionary process using multiple individual observations (e.g., phenotypic measurements) and species-level phylogenetic trees. While we do not develop a new quantitative genetic model of variance evolution (but see "Discussion"), the purpose of our approach is to test hypotheses about the distribution of variances in extant species in a phylogenetic framework. We use Brownian motion and Ornstein–Uhlenbeck processes to model the evolution of intraspecific variances and Brownian motion to model the evolution of phenotypic means. We implement a Markov Chain Monte Carlo (MCMC) algorithm to estimate parameters in the JIVE model and provide a Bayesian framework to compare alternative evolutionary hypotheses. We perform extensive simulations to assess the accuracy and precision with which JIVE can estimate parameters and to evaluate the model selection procedure. We further provide an empirical example to show the application of JIVE for macroevolutionary studies and use data on life-history traits in the Eriogonoideae (buckwheat family, Polygonaceae) to test the differential evolution of intraspecific variability of the climatic niche in this subfamily. Finally, we explain the limitations and advantages of JIVE and outline some future directions for its extension.

Methods and Data

A Hierarchical Bayesian Approach

The JIVE model is structured into three levels: (1) the likelihood level, which models species-specific trait distributions; (2) the prior level, which models evolution of trait means and variances while accounting for phylogenetic dependencies; and (3) the hyperprior level, which allows Bayesian estimation of the parameters of the priors (Fig. 1). The model is implemented using an MCMC algorithm to jointly estimate all parameters and perform model selection.

Likelihood level.—Let us consider a phylogenetic tree with N tips, each corresponding to a species with labels $1, 2, \ldots, N$.

For each species i a sample of trait values is indicated by $\boldsymbol{x_i} = x_i^1, \ldots, x_i^{K_i}$ where $K_i \geq 2$, that is, at least two observations are required for each species. This restriction was imposed to allow the estimation of a species-specific variance in trait values (see below). If some species are not represented by at least two observations, it is possible to replace the trait variance for these species by, for instance, the mean trait variance present in all species with $K_i \geq 2$ or with the trait variance available for closely related species. Alternatively, variances could be sampled from their prior (BM, WN, OU or OUM) iteratively through MCMC. The complete set of observations for N species will be denoted as X and the vector of number of observations for each species is K. We assume $\boldsymbol{x_i}$ to be a sample from

Downloaded from https://academic.oup.com/sysbio/article-abstract/65/3/417/2468958 by UB Leipzig user on 25 October 2019

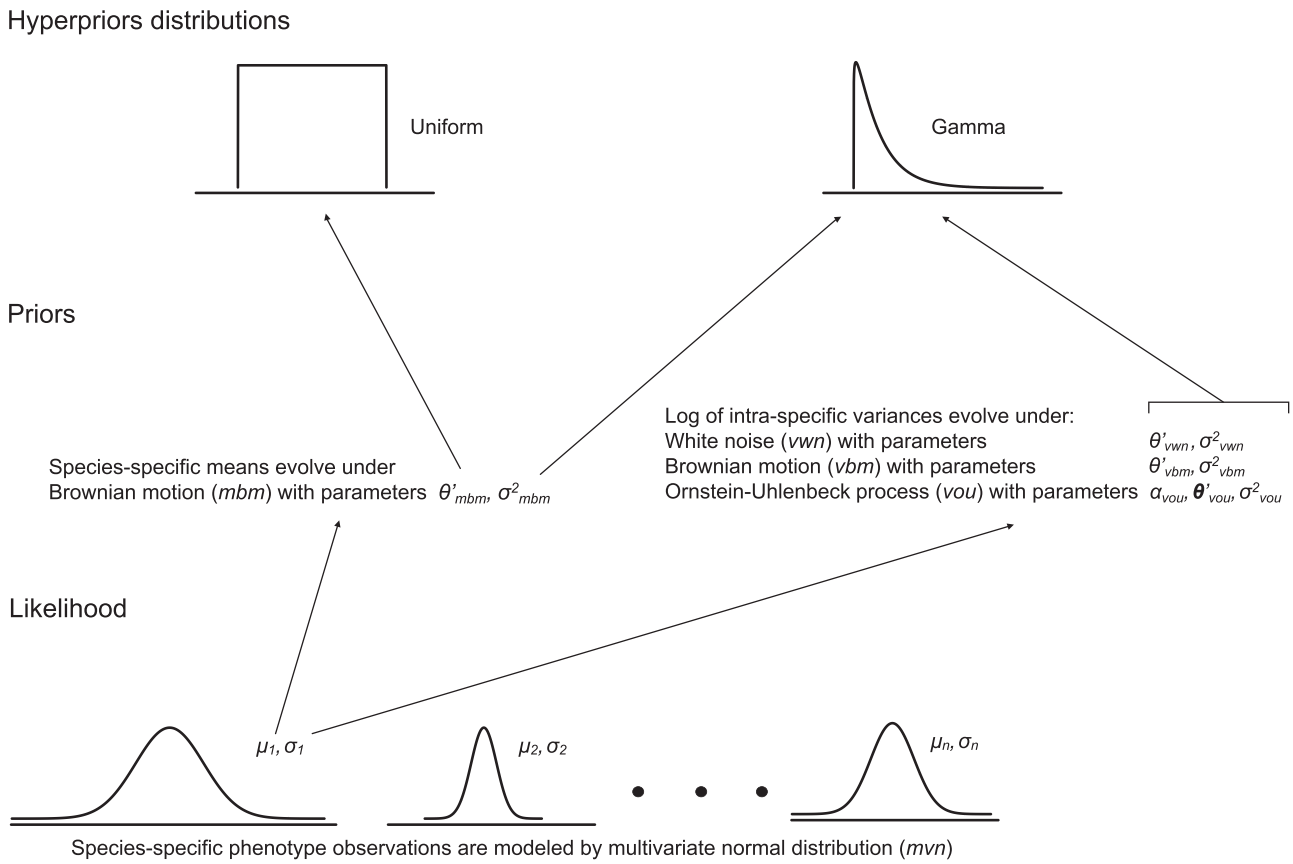

FIGURE 1. Conceptual representation of the hierarchical Bayesian model. The schematic representation includes three levels—likelihood, priors, and hyperpriors. The schema should be read from the bottom to the top. Arrows depict which parameters enter the upper levels of the hierarchy.

a normal distribution with mean μ_i and variance σ_i^2. Therefore, for each species, we can model the probability of observing a sample $\boldsymbol{x_i}$ given the values of μ_i and σ_i^2 as a normal probability density function:

$$P(\boldsymbol{x_i}|\mu_i,\sigma_i^2)=\prod_{k=1}^{K_i}\frac{1}{\sqrt{2\pi\sigma_i^2}}\times\exp\left(-\frac{(x_i^k-\mu_i)^2}{2\sigma_i^2}\right). \quad (1)$$

The likelihood for a set of N species can be calculated as:

$$P(X|\boldsymbol{\mu},\boldsymbol{\sigma^2})=\prod_{i=1}^{N}P(\boldsymbol{x_i}|\mu_i,\sigma_i^2) \quad (2)$$

where $\boldsymbol{\mu} = \mu_1,\ldots,\mu_n$ and $\boldsymbol{\sigma^2} = \sigma_1^2,\ldots,\sigma_n^2$ are the vectors of species-specific means and variances, respectively (Fig. 1). The evolutionary relationships among the N taxa are described by the rooted, time-calibrated phylogenetic tree that is considered to be known without errors (but see "Discussion"). The evolution of the N means and variances is, therefore, influenced by the phylogenetic relationships among the taxa. We estimate these vectors by defining appropriate priors that consider the underlying phylogeny.

TABLE 1. Notations used in the manuscript to denote parameters of the JIVE model and their biological meaning

Biological meaning	Level in JIVE	Mathematical notation
Species-specific means	Likelihood	μ_i ($\boldsymbol{\mu}$)
Species-specific variances	Likelihood	σ_i^2 ($\boldsymbol{\sigma^2}$)
Root state of the species means	Prior	θ'_{mbm}
Evolutionary rate of the species means	Prior	σ^2_{mbm}
Strength of selection on the species variances	Prior	α_{vou}
Evolutionary rate of the species variances	Prior	σ^2_{vou} or σ^2_{vbm}
Root state of the species variances	Prior	θ'_{vou} or θ'_{vbm}
Optimum value of the species variances	Prior	$\boldsymbol{\theta}_{\mathrm{vou}}$

Prior level

Evolution of species means.—Let us first consider the evolution of species-specific means $\boldsymbol{\mu}$ (mbm prior, stands for mean Brownian motion). For simplicity, we assume that the evolution of species means follows a Brownian motion process with a single evolutionary rate parameter σ^2_{mbm} (Felsenstein 1985), describing the rate at which species-specific means change through time (Table 1). This can be easily modified

Downloaded from https://academic.oup.com/sysbio/article-abstract/65/3/417/2468958 by UB Leipzig user on 25 October 2019

to incorporate other models of trait evolution (see "Discussion"). The ancestral state θ'_{mbm} is the starting point of the stochastic processes at the root of the tree. The phylogenetic structure is incorporated through the variance–covariance matrix C, which is a $N \times N$ matrix representing the distances between the most recent common ancestor of each pair of species and the root of the tree (Hansen 1997b; Rohlf 2001). Thus, the prior probability of the vector of species means ($\boldsymbol{\mu}$; equation (2)) can be expressed as a multivariate normal probability density function:

$$P(\boldsymbol{\mu}|\sigma^2_{\text{mbm}}, \theta'_{\text{mbm}}) = \frac{1}{\sqrt{2\pi^n \sigma^2_{\text{mbm}}|C|}} \exp\left(-\frac{1}{2}(\boldsymbol{\mu} - \theta'_{\text{mbm}})^T \sigma^2_{\text{mbm}} C^{-1} (\boldsymbol{\mu} - \theta'_{\text{mbm}})\right) \quad (3)$$

and C is assumed to be constant given that the phylogenetic tree is fixed.

Evolution of species phenotypic variances.—We now consider the evolution of species-specific variances $\boldsymbol{\sigma^2}$ taking into account the phylogenetic relationships among the species. We assume that the evolution of trait variances can be modeled in a similar way to the evolution of trait means. We use the BM process (vbm prior, which stands for variance Brownian motion; a similar notation will be used for the other models described below) and the OU process (vou prior) to model the evolution of phenotypic variances of species (Hansen and Martins 1996; Hansen 1997a). Additionally, we implemented the white noise model (vwn prior), which assumes that variances evolve independently from the underlying phylogenetic tree. The species-specific variances cannot be negative (Roughgarden 1972) with chi-squared sampling distribution, whereas WN, BM and OU processes are typically unbounded with respect to 0. Thus, we use these stochastic processes to model an evolution of log-transformed variances instead of variances of a natural scale. Alternative approaches based on geometric Brownian motion (GBM) and Cox–Ingersoll–Ross (CIR) processes are outlined in the "Discussion".

Let $\boldsymbol{\psi}$ be the vector of log-transformed species-specific variances, $\boldsymbol{\psi} = \log(\boldsymbol{\sigma^2})$. Due to the absence of trend and of equilibrium value, the BM process would be applicable to clades undergoing species diversification or ecological expansion with no selective force acting on the species-specific variance (i.e., some species will have a small phenotypic variance and some a large one). The expansion of the BM process to a multivariate case of N taxa leads to a multivariate normal density function for the prior probability of the species-specific log-variances $\boldsymbol{\psi}$:

$$P(\boldsymbol{\psi}|\sigma^2_{\text{vbm}}, \theta'_{\text{vbm}}) = \frac{1}{\sqrt{2\pi^n \sigma^2_{\text{vbm}}|C|}} \exp\left(-\frac{1}{2}(\boldsymbol{\psi} - \theta'_{\text{vbm}})^T \sigma^2_{\text{vbm}} C^{-1} \boldsymbol{\psi} - \theta'_{\text{vbm}})\right) \quad (4)$$

where the phylogenetic structure is incorporated through the variance–covariance matrix C; σ^2_{vbm} is the evolutionary rate of the species log-variances; and θ'_{vbm} is the root state of the species log-variances. The WN model is obtained by setting the off-diagonals in the variance–covariance matrix C (Equation 4) to 0.

The mean value can change through time and tends toward the optimum that remains unchanged. This pattern allows the testing of several distinct hypotheses or at least the investigation of whether the evolution of variances is following specific trajectories during the evolutionary history of the species as illustrated in Figure 2. Furthermore, modeling two selective regimes in different parts of the tree allows a mixture of these processes and could represent the evolution of a generalist or specialist species that is driven by a particular morphological or physiological adaptation (Fig. 2d). Alternatively, a similar pattern could in principle appear as a result of completely neutral processes—for example, mutation rate evolving as a correlated trait to some life-history character or decrease in dispersal rates resulting in increased genetic isolation and speciation. Finally, the observed pattern may be a result of a mixture of neutral and adaptive processes acting differently on clades in a tree. We relax the OU model to allow more than one selective regime (see Hansen 1997a; Butler and King 2004) and consider OU as an alternative model to the BM and WN models. In our implementation, the assignment of selective regimes to the branches of a phylogeny is defined prior to the analysis (detailed below).

The prior probability of the species log-variances $\boldsymbol{\psi}$ under the OU model also follows a multivariate normal density function:

$$P(\boldsymbol{\psi}|\alpha_{\text{vou}}, \sigma^2_{\text{vou}}, \boldsymbol{\theta}_{\text{vou}}) = \frac{1}{\sqrt{2\pi^n \sigma^2_{\text{vou}}|C|}} \exp\left(-\frac{1}{2}(\boldsymbol{\psi} - W_{\text{vou}}\boldsymbol{\theta}_{\text{vou}})^T \sigma^2_{\text{vou}} C^{-1} (\boldsymbol{\psi} - W_{\text{vou}}\boldsymbol{\theta}_{\text{vou}})\right) \quad (5)$$

where α_{vou} is the strength of selection expressed in 1/(branch lengths units), σ^2_{vou} is the evolutionary rate and $\boldsymbol{\theta}_{\text{vou}}$ is the vector of optima for the species log-variances, which also includes the root state θ'_{vou}. Finally, W_{vou} is the weight matrix and we followed the procedure described in Butler and King (2004) to calculate W_{vou} and paint the different optima on the branches of the tree.

Compared to BM, the OU model includes two additional parameters—the strength of selection, α_{vou}, acting on species log-variances and the optima themselves for the species log-variances, $\boldsymbol{\theta}_{\text{vou}}$. The number and distribution of optima on the tips of a phylogeny should reflect a biological hypothesis about a discrete factor or trait that influences the evolution of species phenotypic log-variances. This is opposed to the model in which there is no difference in optimal log-variance between the species bearing different states of

Downloaded from https://academic.oup.com/sysbio/article-abstract/65/3/417/2468958 by UB Leipzig user on 25 October 2019

such a discrete trait. The mapping of selective regimes on a phylogeny can be obtained from the ancestral reconstruction of categorical traits and their subsequent stochastic mapping on the branches of a phylogeny (Huelsenbeck et al. 2003; Bollback 2006).

Hyperprior level.—We used uniform priors for the root state of the species mean θ'_{mbm} ($\mathcal{U}[-10^4, 10^4]$) and for the root-state of the species log-variances $\theta'_{\text{vou, vbm, vwn}}$ ($\mathcal{U}[-10, 10]$). We chose a gamma prior for evolutionary rates (σ^2_{mbm},σ^2_{vou},σ^2_{vbm},σ^2_{vwn}) and for strength of selection (α_{vou}) with a shape parameter of 1.1 and a scale parameter of 5. Finally, for optimal log-variances $\boldsymbol{\theta}_{\text{vou}}$, we implemented a uniform prior distribution $\mathcal{U}[-10, 10]$.

Sampling Algorithm and Implementation

We implemented the hierarchical Bayesian model using an MCMC with an acceptance ratio based on the posterior:

$$\underbrace{P(\boldsymbol{\mu}, \boldsymbol{\psi}, \sigma^2_{\text{mbm}}, \theta'_{\text{mbm}}, \sigma^2_{\text{vwn}}, \theta'_{\text{vwn}}|X)}_{\text{posterior}} \propto \underbrace{P(X|\boldsymbol{\mu}, \boldsymbol{\sigma^2})}_{\text{likelihood}} \underbrace{P(\boldsymbol{\mu}|\sigma^2_{\text{mbm}}, \theta'_{\text{mbm}})}_{\text{prior mbm}} \underbrace{P(\boldsymbol{\psi}|\sigma^2_{\text{vwn}}, \theta'_{\text{vwn}})}_{\text{prior vwn}} \underbrace{P(\sigma^2_{\text{mbm}})P(\theta'_{\text{mbm}})P(\sigma^2_{\text{vwn}})P(\theta'_{\text{vwn}})}_{\text{hyperpriors}} \quad (6)$$

with WN prior, then

$$\underbrace{P(\boldsymbol{\mu}, \boldsymbol{\psi}, \sigma^2_{\text{mbm}}, \theta'_{\text{mbm}}, \sigma^2_{\text{vbm}}, \theta'_{\text{vbm}}|X)}_{\text{posterior}} \propto \underbrace{P(X|\boldsymbol{\mu}, \boldsymbol{\sigma^2})}_{\text{likelihood}} \underbrace{P(\boldsymbol{\mu}|\sigma^2_{\text{mbm}}, \theta'_{\text{mbm}})}_{\text{prior mbm}} \underbrace{P(\boldsymbol{\psi}|\sigma^2_{\text{vbm}}, \theta'_{\text{vbm}})}_{\text{prior vbm}} \underbrace{P(\sigma^2_{\text{mbm}})P(\theta'_{\text{mbm}})P(\sigma^2_{\text{vbm}})P(\theta'_{\text{vbm}})}_{\text{hyperpriors}} \quad (7)$$

with BM prior, and

$$\underbrace{P(\boldsymbol{\mu}, \boldsymbol{\psi}, \sigma^2_{\text{mbm}}, \theta'_{\text{mbm}}, \alpha_{\text{vou}}, \sigma^2_{\text{vou}}, \boldsymbol{\theta}_{\text{vou}}|X)}_{\text{posterior}} \propto \underbrace{P(X|\boldsymbol{\mu}, \boldsymbol{\sigma^2})}_{\text{likelihood}} \underbrace{P(\boldsymbol{\mu}|\sigma^2_{\text{mbm}}, \theta'_{\text{mbm}})}_{\text{prior mbm}} \underbrace{P(\boldsymbol{\psi}|\alpha_{\text{vou}}, \sigma^2_{\text{vou}}, \boldsymbol{\theta}_{\text{vou}})}_{\text{prior vou}} \underbrace{P(\sigma^2_{\text{mbm}})P(\theta'_{\text{mbm}})P(\sigma^2_{\text{vou}})P(\alpha_{\text{vou}})P(\boldsymbol{\theta}_{\text{vou}})}_{\text{hyperpriors}} \quad (8)$$

with OU prior (Fig. 1). We used sliding-window proposals for most model parameters, thus yielding symmetric updates and a constant Hastings ratio (Ronquist et al. 2012). We updated the species-specific log-variances $\boldsymbol{\sigma^2}$, evolutionary rates ($\sigma^2_{\text{mbm,vou,vbm,vwn}}$), and strength of selection (α_{vou}) parameters using a multiplier proposal (Ronquist and Huelsenbeck 2003), while correcting the Hastings ratio accordingly.

We compared the fit of alternative JIVE models using marginal likelihoods (L_{TI}) obtained by thermodynamic integration (TI; Lartillot and Philippe 2006; Xie et al. 2011). TI requires an MCMC sample to be drawn from a series of distributions ranging from the posterior to the prior at the two extremes of the MCMC path. We generated the path by raising the likelihood ratio to the power of a range of values $\beta \in (0, 1)$, obtained by 10 evenly spaced quantiles of a beta distribution $\mathcal{B}(0.3, 1.0)$ (Xie et al. 2011). We raised to the power of β only the vbm (or vou, vwn) term of Equation (6) (or Equations (7), (8)), whereas the likelihood and the mbm terms were not altered through the TI path. Bayes Factors ($\text{BF} = 2(\log L_{\text{TI}}(M_1) - \log L_{\text{TI}}(M_0))$) were calculated to compare the marginal likelihood of the correct model (i.e., used to simulate the data) against the alternative models (Kass and Raftery 1995). We considered $\text{BF} > 2$ and $\text{BF} > 6$ as indicating moderate and strong evidence for a model, respectively. We measured the accuracy of model selection under increasingly conservative thresholds. We selected the best-fitting model as the one with the smallest marginal likelihood ($\text{BF}_{\text{threshold}} = 0$). We preferred more complex models only when they had BF support greater than 2 log units ($\text{BF}_{\text{threshold}} > 2$), but also report when support was greater then 6 log units ($\text{BF}_{\text{threshold}} > 6$).

The JIVE models were implemented in R, with the code available for download at http://www.unil.ch/phylo/bioinformatics/jive and as Supplementary Material available on Dryad at http://dx.doi.org/10.5061/dryad.n4vp0.

Data Simulations

We simulated trees under a pure-birth model with $N = 50$ species unless otherwise specified and root-to-tip length scaled to one (phytools package, Revell 2012). We then used these trees to simulate evolution of a trait with species-specific means and variances according to different evolutionary models. The species-specific mean trait values ($\boldsymbol{\mu}$) were obtained under a BM model (parameters set to $\theta_{\text{mbm}} = 350$ and $\sigma^2_{\text{mbm}} = 0.5$), whereas the respective variances ($\boldsymbol{\sigma^2}$) were simulated under either WN, BM or OU models. We then sampled multiple

Downloaded from https://academic.oup.com/sysbio/article-abstract/65/3/417/2468958 by UB Leipzig user on 25 October 2019

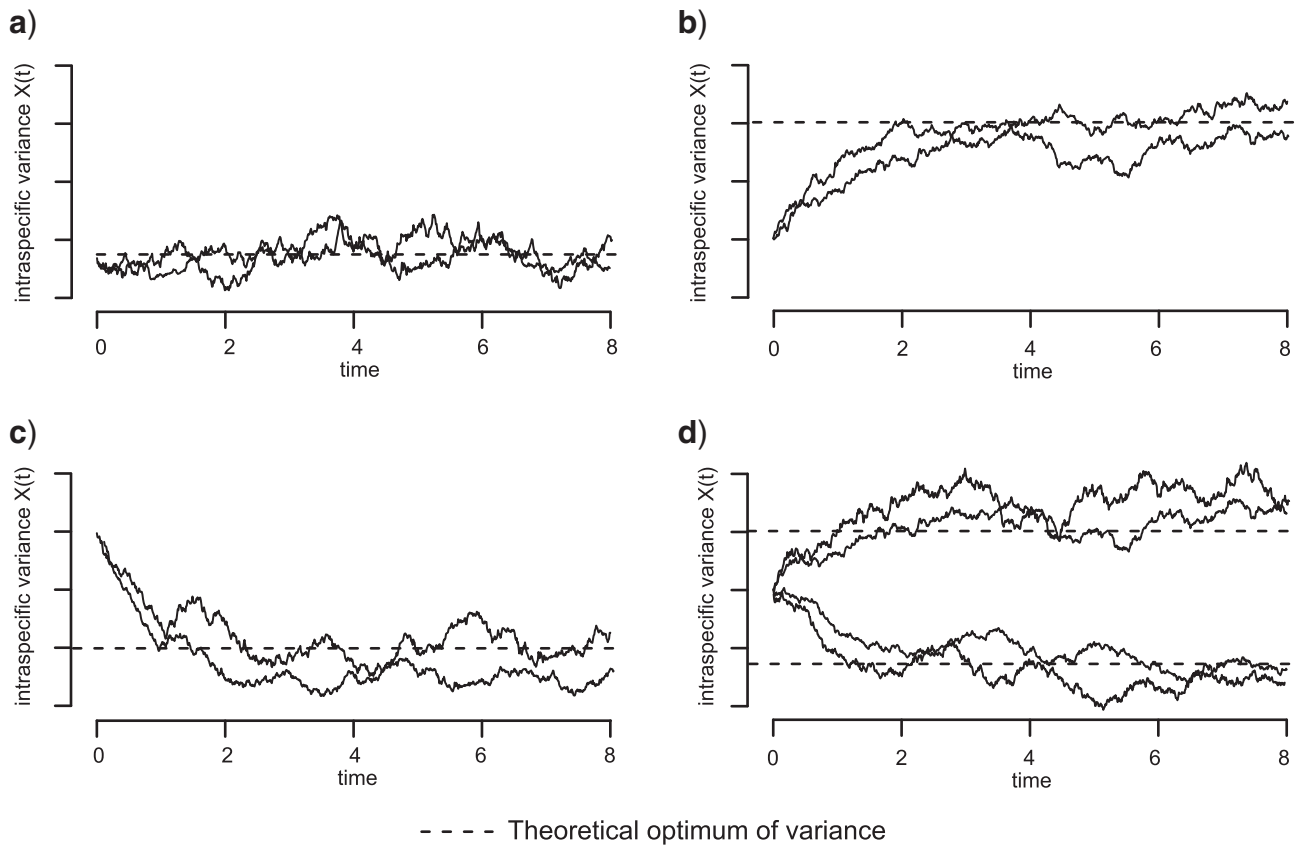

FIGURE 2. Stochastic processes for modeling evolution of intraspecific variances. a) Scenario in which mean variance does not change with time. b) Scenario in which mean variance increases with time as, for example, during an invasion to a new envi ronment; c) Adaptive diversification scenario in which mean variance decreases with time due to, for example, resource partition between congeners; d) Concurrent specialization and generalization between two species due to specific life-history or morphological traits or environment constraints.

observations from normal distributions $\mathcal{N}(\boldsymbol{\mu}, \boldsymbol{\sigma}^2)$ with the number of observations drawn from a Poisson distribution with mean 20 ($K_i = \max[2, \mathcal{P}(20)]$) unless specified otherwise.

We generated species-specific variances (parameter values are detailed below) under WN, BM, OU with a single optimum (OU1) and OU with two optima (OUM) using the OUwie package (Beaulieu et al. 2012) and our own code. The OUM model requires each extant species to be attributed to one of two selective regimes. We simulated these regimes by creating groups of different sizes (from three to eight species), attributing one regime to each group and then randomly assigning these groups to extant species. We then used an equal rate model of discrete trait evolution (ape package, Paradis et al. 2004) to run stochastic mapping in phytools (Revell 2012).

We explored different properties of the JIVE model by varying parameters for the evolution of species-specific variances. Specifically, we:

(1) assessed the ability of our model to accurately recover model parameters by setting different evolutionary rates σ^2, strength of selection α and optima $\boldsymbol{\theta}_{\text{vou}}$ for the evolution of species-specific variances (panel (a) in Table 2). The total numbers of simulation settings were 3, 3, 9, and 18 for WN, BM, OU1, and OUM, respectively;

(2) evaluated the effect of tree size ($N = 50, 100, 200$) and the mean number of observations per species ($K_i = 10, 50, 100$) on the precision of parameter estimates (panel (b) in Table 2). The total numbers of simulation settings were 9 for OU1 and 9 for OUM;

(3) inspected the accuracy of model selection under a range of parameter values (panel (c) in Table 2). The total numbers of simulations settings were 2, 2, 4, and 8 for WN, BM, OU1, and OUM, respectively.

We simulated 10 independent replicates under each simulation setting, which resulted in a total of 670 datasets.

Statistical Evaluation

All simulations for parameter estimation were run for 2,000,000 generations, with a burn-in phase of 500,000. The MCMC chains for model comparison were run for 6,000,000 generations with a burn-in phase of 1,000,000. Efficient chain mixing and effective sample

Downloaded from https://academic.oup.com/sysbio/article-abstract/65/3/417/2468958 by UB Leipzig user on 25 October 2019

TABLE 2. Parameter settings used for simulating datasets to explore: (a) accuracy of parameter estimates; (b) effect of tree size and number of observations; and (c) accuracy of model selection

	Parameter	BM and WN	OU1	OUM
(a)	σ^2	0.1, 0.2, 0.5, 1, 2, 5	0.1, 1, 2, 5	0.1, 1, 2, 5
	θ'	1	1	1
	α		0.1, 1, 2, 5	0.1, 1, 2, 5
	θ_1		1	0.5
	θ_2			1, 1.5, 3
(b)	N		50, 100, 150	50, 100, 150
	K		10, 50, 100	10, 50, 100
	σ^2		1	1
	θ'		1	1
	α		2	2
	θ_1		1	0.5
	θ_2			1.5
(c)	σ^2	0.5, 2	1, 2	1, 2
	θ'	1	1	1
	α		1, 2	1, 2
	θ_1		3	2
	θ_2			4, 6

Note: Simulations were done by using pairwise combinations of all parameters with 10 replicates each.

size were assessed by examining the log files in Tracer (Rambaut and Drummond 2007). Sampled parameters were summarized across 10 replicates as average modal values, average 95% highest posterior densities (95% HPD) and average relative errors to assess model accuracy, precision, and bias. For accuracy in model comparison, we calculated how many times the correct model was preferred against other models based on BF tests.

Life-History Traits in Eriogonoideae

We used a dated phylogeny of 68 Eriogonoideae species (Polygonaceae) (see Kostikova et al. 2013, for details about the data) to test whether a life-history trait (i.e., annual vs. perennial) influences the evolution of intraspecific variation in the climatic niches of species. To estimate intraspecific variation, we collected multiple occurrence records for each species (on average 358, min = 4, max = 2911) from CalFlora, Consortium of California Herbaria, and GBIF databases and extracted bioclimatic variables for each occurrence record from the WorldClim dataset (Hijmans et al. 2005). To reduce the collinearity among variables, the extracted bioclimatic values were compressed into the first three principal components that accounted for most of the variance in the data. These PC values were used to construct an input table for the JIVE model. We identified four competing hypotheses to understand whether this life-history trait shapes the evolution of intraspecific variance. The null hypothesis assumed no phylogenetic component in the evolution of intraspecific variance (WN). The first alternative hypothesis implied that evolution of intraspecific variances follow a Brownian motion model (BM), the second alternative hypothesis assumed evolution of intraspecific variance with no difference in variance optima between annual and perennial species (OU1), and the third alternative hypothesis (OUM) allowed for two different variance optima for the two life-history classes. The OUM hypothesis requires an explicit reconstruction of ancestral life-history classes along the branches of the phylogeny. We used the ape package (Paradis et al. 2004) to estimate the transition rates between life-history classes and a stochastic mapping approach to transform the estimated per-node probabilities into branch proportions (Huelsenbeck et al. 2003; Bollback 2006; Revell 2012). All analyzes were run on a sample of 10 stochastic maps and the results were averaged across the different realizations of the stochastic maps. We performed marginal likelihood estimation to compare the fit of different JIVE models (WN, BM, OU1, OUM) and subsequently estimated the parameters under the best fitting model.

RESULTS

Simulations and Statistical Evaluation

The values of species-specific means and variances are well recovered by the JIVE model. Across all models and all simulations, the average relative error of estimated species means and their standard deviations are smaller than 0.0002 (Supplementary Fig. S1). The credible intervals around the posterior estimates of $\boldsymbol{\mu}$ are consistently narrow across simulations (95% HPD: 349.66–350.50). We do not detect any systematic bias in the estimated species means under any of the simulation settings (Supplementary Fig. S1). Similarly, species variances $\boldsymbol{\sigma^2}$ are estimated accurately. The relative error is on average smaller than |0.1|. The estimated species variances are unbiased and not influenced by the parameters of the priors (Supplementary Fig. S1). The species variances and means are unbiased and accurately estimated (Supplementary Fig. S1).

The parameters of the mbm prior (θ'_{mbm} and σ^2_{mbm}) are consistently well-estimated across different simulations and parameter settings (Supplementary Fig. S2), with an average relative error on θ'_{mbm} smaller than |0.0002| and narrow credible intervals (95% HPD: 349.36–350.69; true value 350). This confirms both the high accuracy and precision of the estimation of θ'_{mbm}. The variance σ^2_{mbm} is accurately estimated across all simulations with an average relative error of |0.07| (Supplementary Fig. S2), and narrow credible intervals (95% HPD: 0.28–0.93; true value 0.5). The estimated mean θ'_{mbm} and variance σ^2_{mbm} of the mbm prior are unbiased with respect to the vbm (or vou) priors (Supplementary Fig. S2).

The JIVE model accurately recovers the evolutionary rate of the species-specific variances (σ^2_{vbm} and σ^2_{vwn}) and root state of the species variances (θ'_{vbm} and θ'_{vwn}) under both the BM and WN priors, with average relative errors smaller than |0.5| (Fig. 3). The estimated species-specific

Downloaded from https://academic.oup.com/sysbio/article-abstract/65/3/417/2468958 by UB Leipzig user on 25 October 2019

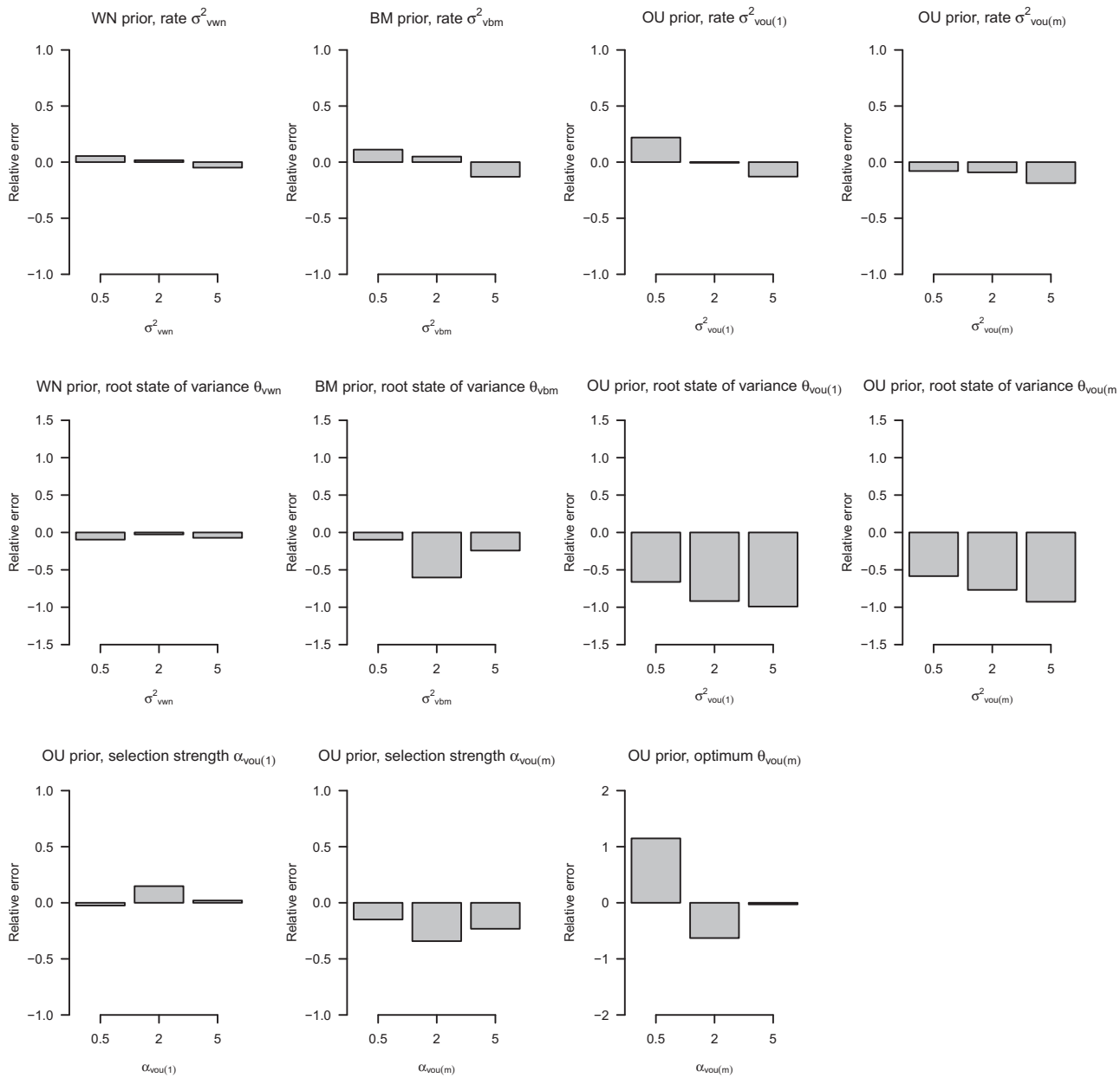

FIGURE 3. Relative errors of the estimated parameters. The shaded bars represent underestimation of the true parameter value and white bars represent overestimation of the true parameter value. The estimates are sorted on the x-axis by either the value of a parameter itself (such as σ^2_{vou} for estimates of σ^2_{vou}) or by another important parameter (such as α_{vou}) to show the interaction between the estimated parameter and this sorting parameter. The relative errors are averaged over the simulated values for all other parameters (Table 2).

variances and ancestral states for these two priors are unbiased with respect to their simulated values and have narrow credible intervals around the posterior estimates (Fig. 4). Similarly, the parameters of the vou prior are well estimated for all parameter settings, except for very small values of α_{vou} and σ^2_{vou} (Fig. 3). On average, and excluding the simulations with a very small α_{vou}, the relative errors on α_{vou}, σ^2_{vou}, and $\boldsymbol{\theta}_{\text{vou}}$ are small (|0.63|, |0.13|, |0.25|, and |0.06|, respectively) and all parameters are recovered with narrow 95% credible intervals (Fig. 4). In general, we observe that estimates of selection on variance α_{vou} are positively biased and that bias increases as the estimated selection strength α_{vou} decreases. The estimates of the other parameters (σ^2_{vou} and $\boldsymbol{\theta}_{\text{vou}}$) do not display any systematic error (Fig. 4).

On average, the precision and accuracy of the parameter estimates increase when the number of observations K_i is larger (Supplementary Fig. S3). For example, when we set the mean sample size K_i to 50 instead of 10, the relative errors of α_{vou}, σ^2_{vou}, and $\boldsymbol{\theta}_{\text{vou}}$ decrease by half. A further increase of the mean sample size K_i improves the accuracy of the parameters only

Downloaded from https://academic.oup.com/sysbio/article-abstract/65/3/417/2468958 by UB Leipzig user on 25 October 2019

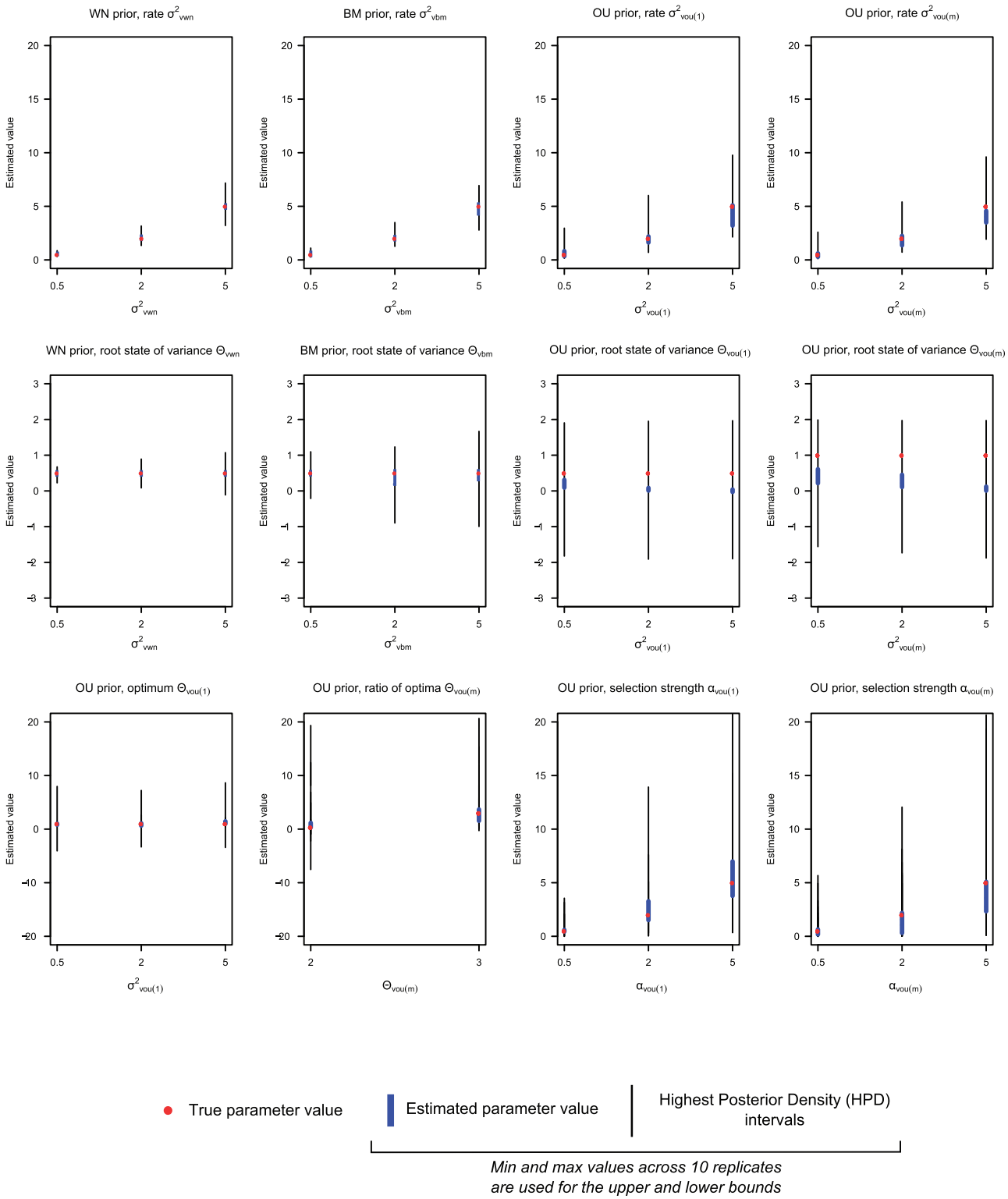

FIGURE 4. The 95% HPD and mean estimates of the parameters. For each graph the results represent the summary across 10 independent replicates: the thick bars are the spread between the minimum and the maximum value of an estimated parameter across 10 replicates; the HPD bars are the minimum value of lower 95% HPD interval and the maximum value of upper 95% HPD interval across 10 replicates; the dot is the true parameter value under which the simulation was run. The estimates are sorted on the *x*-axis by either the value of a parameter itself (such as σ^2_{vou} for estimates of σ^2_{vou}) or by another important parameter (such as α_{vou}) to show the interaction between the estimated parameter and this sorting parameter.

Downloaded from https://academic.oup.com/sysbio/article-abstract/65/3/417/2468958 by UB Leipzig user on 25 October 2019

TABLE 3. Accuracy of model selection based on Bayes factors calculated as a percentage of models correctly identified given different thresholds

	True model	Compared with	$BF_{threshold} > 0$	$BF_{threshold} > 2$	$BF_{threshold} > 6$
(a)	BM	WN	100.0	100.0	90.0
	WN	BM	89.5	89.5	78.9
	OU1	BM or WN	80.4	64.6	36.1
	OUM	BM, WN or OU1	61.1	50.0	32.9
			$BF_{threshold} > 0$	$BF_{threshold} > -2$	$BF_{threshold} > -6$
(b)	BM	OU1	85.0	95.0	100.0
	WN	OU1	70.0	75.0	85.0
	OU1	OUM	93.4	93.4	93.4

Notes: The true model was the model used to create the simulated data. The marginal likelihood of this true model was then compared against the other models. The comparisons is divided into accuracy against (panel (a)) simpler and (panel (b)) more complex models than the true model.

slightly (Supplementary Fig. S3). Larger trees can also improve the accuracy of parameter estimation, especially α_{vou} (Supplementary Fig. S3).

Model selection based on TI is capable of finding the correct model in more than 80% of the cases with BF thresholds 0 and 2 for the simpler models used in the simulations (i.e., BM, WN and OU1; Table 3). Under BF threshold of 6, model selection is more conservative and tends to favor simpler models over more complex ones (Table 3), even if the model used to perform the simulations was more complex.

Life-History Traits in Eriogonoideae

The first three PCA axes explain 38.54%, 35.53%, and 8.96% of variation in the climatic niche. The axis PC1 is most strongly correlated with precipitation of the wettest season and temperature of the coldest season (BIO1, BIO6, BIO8, and BIO9 WorldClim variables), whereas PC2 represents mainly seasonality and isothermality (BIO2, BIO3, BIO4, BIO7, BIO12, and BIO19), and PC3 represents precipitation seasonality and precipitation of the driest season (BIO8, BIO14, BIO17, and BIO18). The BM model of variance evolution is rejected across all PC axes (Table 4 and Supplementary Table S1). In contrast, the WN model is preferred for the axes PC2 and PC3, with a strong BF > 6 in the case of the latter axis. This suggests that the evolution of the species-specific variances on these two axes is not associated with the phylogenetic relationships found between the species. In contrast, the PC1 is strongly favoring a OU-type model of evolution for the species-specific variances with BF > 3.3 against the simpler models, although the differences between OU1 and OUM is only marginally better for OUM BF < 2 (Table 4).

The estimated parameters indicate that in PC1, after transforming back the log-variances into their original scale, the intraspecific variance is more than three times as large for perennial species compared with annual species (PC1: θ_a = 1.22 [HPD: 0.49–3.63] and θ_p = 4.46 [HPD: 1.16–24.78]; Fig. 5 and Supplementary Fig. S2). Figure 5 also shows the scatter plot of the values sampled from the posterior distribution directly on the θ_a/θ_p plane. The fraction of points falling above the diagonal line indicates a clear support in favor of different optima for perennial and annual species.

TABLE 4. Bayes factors between evolutionary models for three climatic axes of Eriogonoideae calculated in JIVE by comparing the marginal likelihood of the best-fitting model against all the others

	BM	OU1	OUM	WN
PC1	3.32	0.41	0	12.16
PC2	6.61	1.08	1.94	0
PC3	18.19	5.36	6.84	0

DISCUSSION

The evolution of intraspecific variation is a long-standing issue in evolutionary biology (Roughgarden 1972; Pianka 1974; Bolnick et al. 2011). Variability in phenotypic data is typically decomposed into the additive genetic variance, which represents the heritable component, and other sources of phenotypic variance. The latter can include, for example, plasticity, nonadditive or environmental variance, and measurement error. At the macroevolutionary level, intraspecific variation is further increased by differences across the geographic range of a species. However, current methods have simplified the components of the phenotypic variability and considered it in the form of correlated mean phenotypes and independently distributed residual deviation (Lynch 1991; Ives et al. 2007; Felsenstein 2008; Revell and Reynolds 2012). In reality, however, the residual deviation likely has a heritable component (Turelli 1984; Lynch and Walsh 1998) and is subject to selective constraints or random evolution (Ackermann and Doebeli 2004). We propose a hierarchical Bayesian solution that overcomes the existing assumption of nonevolving intraspecific variance through a framework to test hypotheses about variance evolution. It further allows simultaneous modeling of the evolution of species mean phenotype

Downloaded from https://academic.oup.com/sysbio/article-abstract/65/3/417/2468958 by UB Leipzig user on 25 October 2019

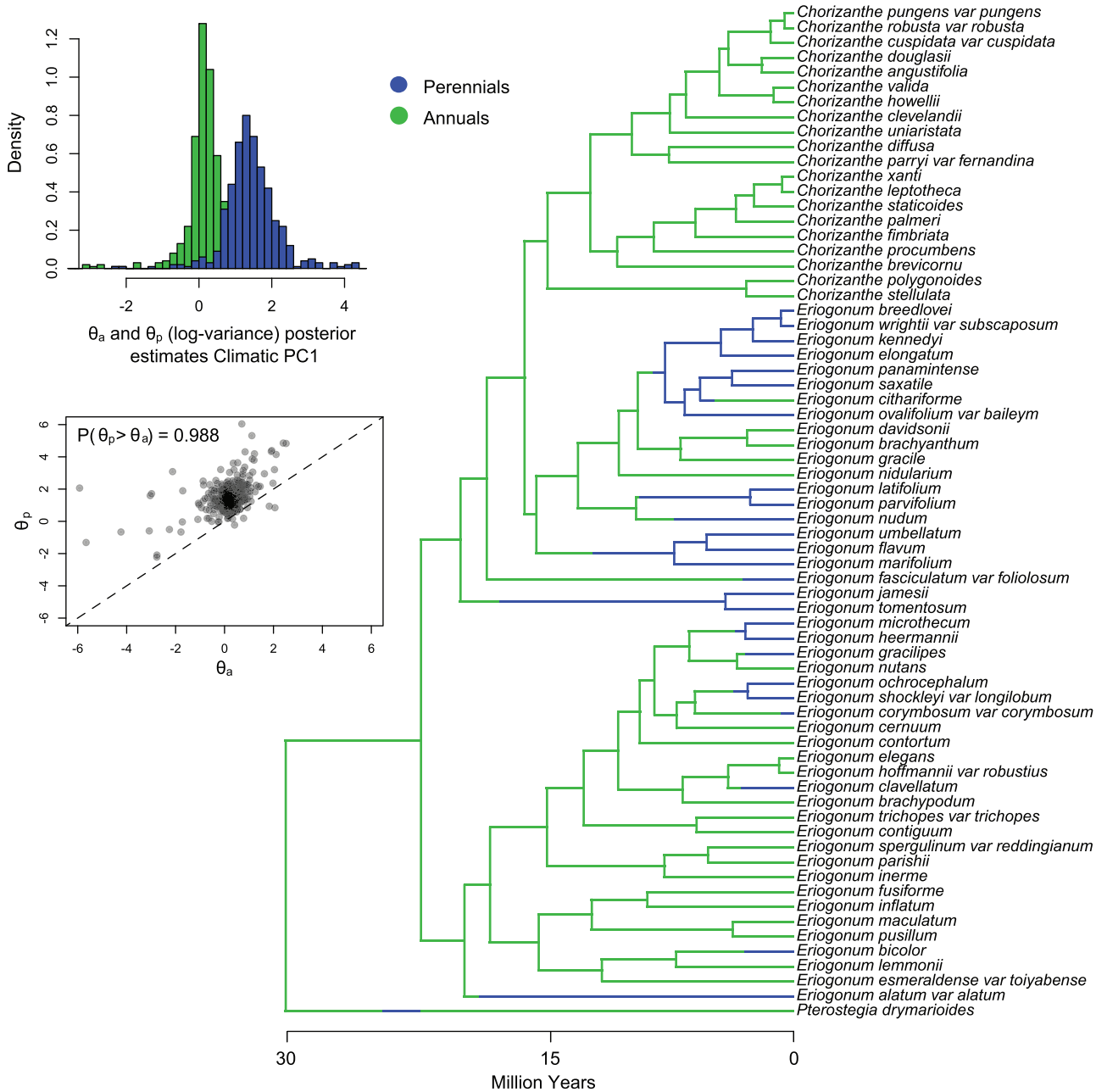

FIGURE 5. Dated phylogeny of Eriogonoideae species and estimated niche variances optima for annual and perennial life-history classes. The dated phylogeny of the 68 Eriogonoideae species and the posterior densities of the estimated optima of intraspecific variances for annual and perennial species. The posterior densities are also represented as a scatter plot of the values directly on the θ_a/θ_p plane, which shows a clear support for $\theta_p > \theta_a$.

and intraspecific variances. We implement three stochastic processes (WN, BM, and OU) to represent different scenarios of the evolution of variances and impose the evolution of species mean phenotypes under the conventional Brownian model. Furthermore, we develop a Bayesian framework for model comparison and apply the proposed method to analyze the evolutionary history of intraspecific variation in the climatic niche of species in the Eriogonoideae. While teasing apart plasticity from genetic variance remains difficult, our model extends current approaches that deal with phylogenetically independent measurement errors and turns the assumption of evolving variances into a testable hypothesis.

Exploring the Behavior of the JIVE Model

We have explored the statistical behavior of our comparative model and an inference framework by analyzing simulated and empirical data. We have also

Downloaded from https://academic.oup.com/sysbio/article-abstract/65/3/417/2468958 by UB Leipzig user on 25 October 2019

examined the sensitivity of our model to the range of model parameters, and the accuracy and precision of parameter estimates based on simulated datasets. We can generally accurately infer the true value of the strength of selection on intraspecific variances.

Overall, we accurately recover σ^2_{vbm} and σ^2_{vou}, although for small values of σ^2_{vbm} or σ^2_{vou} the true parameter values are more difficult to estimate accurately and are usually overestimated. The accuracy of $\boldsymbol{\theta}_{vou}$ depends on the value of α_{vou}, that is, when selection is stronger (large α_{vou}), then all $\boldsymbol{\theta}_{vou}$ values are estimated more accurately. This is expected because when the selection strength is substantial, it forces the trait (in this case the variance) toward the optimum $\boldsymbol{\theta}_{vou}$ and maintains it near the optimal value (Hansen 1997a). The parameters σ^2_{vbm} or σ^2_{vou}, in contrast, do not alter the accuracy of the estimation of $\boldsymbol{\theta}_{vou}$. Larger values of σ^2_{vou} will increase the stationary variance of the OU process, which is calculated as $\alpha_{vou}/(2*\alpha)$. The increased variance of the sampled data around the optimum does result in a wider posterior estimate for θ_{vou}, but we observed that the mean value for this parameter is well estimated in our simulations (Figure 4). Finally, tree size and the number of observations per species positively influence the precision and accuracy of the parameter estimates, showing that the estimation of variances is sensitive to sample size.

Bayesian model selection via TI has sufficient power to correctly find the true model (Table 3). The more complex model (OUM) is more prone to misclassification (incorrect rejection) than simpler models under a conservative BF threshold (Table 3). Therefore, in empirical studies a smaller selection threshold (e.g., $BF_{threshold} > 2$) might be a better choice because it yields higher average accuracy (Tables 3 and 4). This may be particularly applicable to cases in which the true difference between OUM optima is small and either evolutionary rateσ^2_{vbm} is large or selection strength α_{vou} is small. In such circumstances, we underestimate the support for the models with larger numbers of parameters (Table 3). This is anticipated, because, under such conditions, the OUM model resembles the BM model, making model selection more difficult.

Life-History Traits in Eriogonoideae

We have illustrated the applicability of our method with an empirical analysis of the climatic tolerances of 68 Californian Eriogonoideae species. We did not use phylogenetic PCA (Revell 2009) on our empirical dataset because this method cannot, so far, accommodate multiple observations per species, which is the main focus of our method. Bayes factors strongly favor non-Brownian evolution of species-specific variances (Table 4 and Supplementary Table S1), yet the inferred scenarios of evolution of intraspecific variance differ depending on the axis of climatic principal components. For the PC2 (seasonality and isothermality) and PC3 axis (precipitation of the driest season), the best fitted model was WN, but with very similar BF values for the OU1 model (at least for PC2; Table 4 and Supplementary Table S1). In contrast, the evolution of intraspecific variance on the PC1 axis is best described by the model with two optima that differ between the life-history classes (Table 4 and Supplementary Table S1). The inferred optimal values of intraspecific variances on the PC1 axes are more than three times larger for perennial species than for annuals, which suggests that perennial species evolve broader climatic tolerances relative to annuals (Figure 5). The OU1 model is, however, not formally rejected in favor of OUM for the PC1 axes, despite the fact that the parameter estimates are clearly different. This result suggests that our approach has moderate power for trees of the size of the Eriogonoideae dataset and this is confirmed by our simulations.

The inferred patterns suggest that two complementary evolutionary processes regulate the evolution of climatic tolerances in Californian erigonoids. First, there is a lack of phylogenetic effects on the evolution of the variance of the PC2 and PC3 axes. These results suggest that the phylogenetic tree does not influence the evolution of the climatic tolerance and could indicate a lack of heritability of the phenotypic variance represented by these two axes. This scenario is consistent with the earlier studies on North American erigonoids (Reveal 1989; Sanchez and Kron 2008; Kempton 2012) and the Californian flora in general (Whittaker 1960; Stebbins and Major 1965; Cole 1967; Evans et al. 2009). Because these multiple radiations occurred possibly simultaneously across different clades, the phylogenetic structure of the resulting niches might be blurred due to convergent evolution (Revell et al. 2008). Consequently, competitive exclusion, common in adaptive radiations (Gavrilets and Losos 2009), may drive the rapid evolution of resource partitioning and niche specialization (Ackermann and Doebeli 2004). Second, broader climatic tolerances in perennial species across PC1 are likely associated with elevational gradients and increasing climatic instability at higher elevations, where many perennial species are found (Kostikova et al. 2013). When environment is characterized by low predictability, species respond with broadened environmental tolerances (MacArthur 1965, 1972). Such a strategy allows broad-niched species a form of bet-hedging to successfully survive harsher years (Philippi 1993).

Advantages and Limitations of the JIVE Model

Decoupling the evolution of intraspecific variance from the evolution of phenotypic means offers several benefits. First, our model allows explicit investigation of the parameters of intraspecific evolution at a macroevolutionary scale, which so far has not been possible. This can help to advance our understanding of how environmental conditions and life-history, morphological and physiological traits impact the evolution of intraspecific variability.

Downloaded from https://academic.oup.com/sysbio/article-abstract/65/3/417/2468958 by UB Leipzig user on 25 October 2019

Second, our framework simultaneously estimates species-specific parameters, such as mean phenotype and intraspecific variances, and clade-specific parameters, such as evolutionary rate, strength of selection, and optima. The estimation of parameters describing the evolution of intraspecific variances could be performed in a maximum likelihood framework to provide a fast way for model testing. However, the hierarchical Bayesian estimation of such parameters has the desirable property of jointly estimating all intraspecific means and variances, thus incorporating the respective uncertainties in the analysis. This should produce results that are more robust and less prone to error propagation (Lartillot and Poujol 2011). Thus, the joint estimation of intraspecific means and variances can be particularly advantageous in comparison to the estimation of evolution of species-specific variances in a conventional framework in which variances are regarded as individual species traits.

Despite certain benefits, the ability to decouple the intraspecific and interspecific components of phenotypic evolution raises some issues. Existing comparative models make a clear connection between the phylogenetic variance–covariance matrix and microevolutionary models (Hansen and Martins 1996). In our case, we speculate that a similar assertion can be made regarding the evolution of intraspecific variance. This assumes that the intraspecific variance is a heritable trait itself, which is a strong assumption to make at this stage. The implementation of the white noise model allows, however, to remove alltogether this assumption as this model forces variance to be independent of the phylogenetic structure. Much work is needed to obtain a clear understanding of how genetic variation changes through various time scales. In this context, new theoretical developments building on, for instance, the house-of-cards model (Turelli 1985) could bring important insights by enabling theoretical predictions for the effect of selection over various timescales as it has recently been shown for gene expression (Hodgins-Davis et al. 2015). However, our model can easily be adapted to a more simple scenario in which intraspecific variance is entirely explained by measurement error or one in which there is no phylogenetic covariance between species-specific variances. Indeed, these two hypotheses can be compared in a framework against more complex scenarios by simply setting to zero the off-diagonals of the variance–covariance matrix in the BM prior for species-specific variances. Furthermore, our models assume a symmetrical inheritance of the intraspecific variances by daughter lineages, which may not be realistic in some cases. However, this limitation could be overcome by describing cladogenetic evolution of variance based on asymmetrical inheritance similarly to models applied in historical biogeography (Ree et al. 2005; Ree and Smith 2008; Goldberg et al. 2011).

Another potential limitation of our model is the fact that identifying the process underlying the evolution of phenotypic variances is even more complex than with phenotypic means, because similar patterns could derive from different evolutionary processes. For example, the observed patterns of climatic niche variance evolution in Eriogonoideae could be generated by the predominantly neutral forces (e.g., demography and geographic speciation) or a mixture of neutral and adaptive processes. Resolving these issues is not straightforward and we need to better connect the population level models with the expected macroevolutionary patterns at a broader scale. The dynamic nature of the adaptive landscapes driving the evolution of phenotypic variances is possibly contrasted by a possibly more static nature at the macroevolutionary scales. This decoupling is challenging but several possible solutions could be envisaged to tackle this issue. For instance, it would be interesting to model the movement of adaptive zones and a hierarchical modeling approach to combine the processes happening at the genetic level and phenotypic level (e.g., Uyeda and Harmon 2014).

Extending the JIVE Model

A promising feature of the proposed Bayesian framework is its flexibility. While the current implementation of the JIVE model makes a number of simplistic assumptions, they are nevertheless easy to overcome by extending the proposed model. For example, we assume: a single model of evolution of species-specific means; a tree topology known without errors; and hyperpriors on posterior distributions are relatively naïve and do not exploit additional biologically relevant information. Below we briefly discuss each of these three assumptions and suggest possible future extensions to the JIVE model.

We limit our current set of models to only three alternative stochastic processes—white noise, Brownian motion, and Ornstein–Uhlenbeck processes. The rationale behind this comes from theoretical ecology research that suggests that these stochastic processes adequately describe the evolutionary change of intraspecific variances (Roughgarden 1972; Hubbell 2001; Kassen 2002; Ackermann and Doebeli 2004; Bolnick et al. 2011). Recent years have seen a rapid growth in a number of available comparative models (Butler and King 2004; O'Meara et al. 2006; Eastman et al. 2011; Beaulieu et al. 2012; Landis et al. 2013b), thus, the first natural extension to the current implementation of JIVE would be incorporation of available models of phenotypic mean evolution. Second, other stochastic processes may be necessary to adequately represent more complex evolutionary histories of intraspecific variance evolution. For example, GBM and CIR, which both have a boundary condition at 0, could be appropriate for the evolution of variances. However, the comparability of multivariate log-normal likelihoods to multivariate normal likelihoods (e.g., BM- and OU-based) remains unexplored and needs additional analysis.

The current implementation assumes a fixed and known time-calibrated tree topology. The naïve way

Downloaded from https://academic.oup.com/sysbio/article-abstract/65/3/417/2468958 by UB Leipzig user on 25 October 2019

to overcome such restriction is to use a representative sample of tree topologies from a Bayesian posterior obtained from, for example, Bayesian phylogeny reconstructing software such as MrBayes or BEAST (Ronquist and Huelsenbeck 2003; Drummond and Rambaut 2007). Also, the JIVE model could be extended to use the joint proposal for both evolutionary histories of a trait and phylogeny (Lartillot and Delsuc 2012; Landis et al. 2013a).

Usage of biologically informative hyperpriors could be highly advantageous. For instance, if multiple fossil records are available and present a common ancestor of the observed extant taxa, the fossil phenotypic measurements can be used as a hyperprior on ancestral variance parameter (Lartillot and Delsuc 2012; Slater et al. 2012), thus adding information to the observed evolutionary patters. Potentially, this can greatly increase the accuracy of the model in predicting reduction or increase in variance through time. In theory, it may also be possible to make a link between the priors' parameters on evolutionary means and variances through an extra hyperprior. This may help to resolve the interplay between the evolution of mean phenotypes and additive genetic variance and potentially help to estimate the selection coefficient. Finally, setting more complex priors borrowed from coalescent theory could provide an interesting link between trait evolution on macroevolutionary and population levels.

Conclusion

The era of Bayesian statistics and MCMC has entered the field of comparative phylogenetics. These approaches provide a flexible framework not only at the level of phylogenetic reconstructions (Huelsenbeck and Ronquist 2001; Drummond and Rambaut 2007; Ronquist et al. 2012), but also at the level of efficient analysis of complex biogeographical histories (Landis et al. 2013a), models of protein and codon evolution (Lartillot and Philippe 2006), and now comparative phylogenetics (Revell and Reynolds 2012). We are hopeful that the framework described here will make yet another step toward increasing the efficiency and scope of comparative models, and boost our ability to disentangle complex macroevolutionary histories.

Supplementary Material

Data available from the Dryad Digital Repository: http://dx.doi.org/10.5061/dryad.n4vp0.

Funding

This work was supported by Swiss National Science Foundation grants 3100A0-122433 and 3100A0-163428 to P.B.P. and N.S., respectively. D.S. acknowledges financial support from Carl Tryggers stiftelse and Wenner-Gren foundation.

Acknowledgments

The Vital-IT facilities of the Swiss Institute of Bioinformatics were used for all computational aspect of this study.

References

Ackermann M., Doebeli M. 2004. Evolution of niche width and adaptive diversification. Evolution 58:2599–2612.
Beaulieu J.M., Jhwueng D.-C., Boettiger C., OMeara B.C. 2012. Modeling stabilizing selection: expanding the OrnsteinUhlenbeck model of adaptive evolution. Evolution 66:2369–2383.
Bollback J.P. 2006. SIMMAP: stochastic character mapping of discrete traits on phylogenies. BMC Bioinform. 7:88.
Bolnick, D.I. 2001. Intraspecific competition favours niche width expansion in Drosophila melanogaster. Nature 410:463–466.
Bolnick D.I., Amarasekare P., Arajo M.S., Brger R., Levine J.M., Novak M., Rudolf V.H.W., Schreiber S.J., Urban M.C., Vasseur D.A. 2011. Why intraspecific trait variation matters in community ecology. Trends Ecol. Evol. 26:183–192.
Bolstad G.H., Hansen T.F., Pelabon C., Falahati-Anbaran M., Perez-Barrales R., Armbruster W.S. 2014. Genetic constraints predict evolutionary divergence in dalechampia blossoms. Philos. T. Roy. Soc. B. 369.
Butler M.A., King A.A. 2004. Phylogenetic comparative analysis: a modeling approach for adaptive evolution. Am. Nat. 164:683–695.
Cole N.H.A. 1967. Comparative physiological ecology of the genus Eriogonum in the Santa Monica Mountains, Southern California. Ecol. Monogr. 37:2–24.
Darwin C. 1859. On the origin of the species by natural selection. Murray.
Drummond A., Rambaut A. 2007. BEAST: Bayesian evolutionary analysis by sampling trees. BMC Evol. Biol. 7:214.
Eastman J.M., Alfaro M.E., Joyce P., Hipp A.L., Harmon L.J. 2011. A novel comparative method for identifying shifts in the rate of character evolution on trees. Evolution 65:3578–3589.
Evans M., Smith S., Flynn R., Donoghue M. 2009. Climate, niche evolution, and diversification of the Bird-Cage Evening Primroses (Onothera, sections Anogra and Kleinia). Am. Nat. 173:225–240.
Felsenstein J. 1985. Phylogenies and the comparative method. Am. Nat. 125:1–15.
Felsenstein J. 2008. Comparative methods with sampling error and within-species variation: contrasts revisited and revised. Am. Nat. 171:713–725.
Garamszegi L.Z., Møller A.P. 2010. Effects of sample size and intraspecific variation in phylogenetic comparative studies: a meta-analytic review. Biol. Rev. 85:797–805.
Gavrilets S., Losos J.B. 2009. Adaptive radiation: contrasting theory with data. Science 323:732–737.
Goldberg E.E., Lancaster L.T., Ree R.H. 2011. Phylogenetic inference of reciprocal effects between geographic range evolution and diversification. Syst. Biol. 60:451–465.
Grant P., Price T. 1981. Population variation in continuously varying traits as an ecological genetics problem. Am. Zool. 21:795–811.
Hansen T.F. 1997a. Stabilizing selection and the comparative analysis of adaptation. Evolution 51:1341–1351.
Hansen T.F. 1997b. Stabilizing selection and the comparative analysis of adaptation. Evolution 1341–1351.
Hansen T.F., Bartoszek K. 2012. Interpreting the evolutionary regression: the interplay between observational and biological errors in phylogenetic comparative studies. Syst. Biol. 61:413–425.
Hansen T.F., Houle D. 2008. Measuring and comparing evolvability and constraint in multivariate characters. J. Evolution. Biol. 21:1201–1219.
Hansen T.F., Martins E.P. 1996. Translating between microevolutionary process and macroevolutionary patterns: the correlation structure of interspecific data. Evolution 1404–1417.
Herrera C.M. 1996. Floral traits and plant adaptation to insect pollinators: a devils advocate approach. Springer, p. 65–87.
Hijmans R.J., Cameron S.E., Parra J.L., Jones P.G., Jarvis A. 2005. Very high resolution interpolated climate surfaces for global land areas. Int. J. Climatol. 25:1965–1978.

Downloaded from https://academic.oup.com/sysbio/article-abstract/65/3/417/2468958 by UB Leipzig user on 25 October 2019

Hodgins-Davis A., Rice D.P., Townsend P.T. 2015. Gene expression evolves under a house-of-cards model of stabilizing selection. Mol. Biol. Evol. 2130–2140.
Hubbell S.P. 2001. The unified neutral theory of biodiversity and biogeography. Princeton (NJ): Princeton University Press.
Huelsenbeck J., Ronquist F. 2001. MrBayes: Bayesian inference of phylogenetic trees. Bioinformatics 17:754–755.
Huelsenbeck J.P., Nielsen R., Bollback J.P. 2003. Stochastic mapping of morphological characters. Syst. Biol. 52:131–158.
Hutchinson G.E. 1978. An introduction to population ecology. New Haven, Connecticut: Yale University Press.
Ives A.R., Midford P.E., Garland T. 2007. Within-species variation and measurement error in phylogenetic comparative methods. Syst. Biol. 56:252–270.
Kass R.E., Raftery A.E. 1995. Bayes factors. J. Am. Stat. Assoc. 90: 773–795.
Kassen R. 2002. The experimental evolution of specialists, generalists, and the maintenance of diversity. J. Evolution. Biol. 15:173–190.
Kempton E.A. 2012. Systematics of Eriogonoideae s. s. (Polygonaceae). Syst. Bot. 37:723–737.
Kostikova A., Litsios G., Salamin N. and Pearman P.B. 2013. Linking life-history traits, ecology, and niche breadth evolution in North American Eriogonoids (Polygonaceae). Am. Nat. 182:760–774.
Lande R. 1976. Natural selection and random genetic drift inphenotypic evolution. Evolution 30:314–334.
Landis M.J., Matzke N.J., Moore B.R. and Huelsenbeck J.P. 2013a. Bayesian analysis of biogeography when the number of areas is large. Syst. Biol. 62:789–804.
Landis M.J., Schraiber J.G., Liang M. 2013b. Phylogenetic analysis using lã©vy processes: finding jumps in the evolution of continuous traits. Syst. Biol. 62:193–204.
Lartillot N., Delsuc F. 2012. Joint reconstruction of divergence times and life-history evolution in placental mammals using a phylogenetic covariance model. Evolution 66:1773–1787.
Lartillot N., Philippe H. 2006. Computing Bayes factors using thermodynamic integration. Syst. Biol. 55:195–207.
Lartillot N., Poujol R. 2011. A phylogenetic model for investigating correlated evolution of substitution rates and continuous phenotypic characters. Mol. Biol. Evol. 28:729–744.
Lynch M. 1991. Methods for the analysis of comparative data in evolutionary biology. Evolution 45:1065–1080.
Lynch M., Walsh B. 1998. Genetics and analysis of quantitative traits. Sunderland (MA): Sinauer.
MacArthur R. 1965. Patterns of species diversity. Biol. Rev. 40:510–533.
MacArthur R. 1972. Geographical ecology. Princeton (NJ): Princeton University Press.
MacArthur R., Levins R. 1964. Competition, habitat selection, and character displacement in a patchy environment. Proc. Natl Acad. Sci. USA 51:1207–1210.
Martins E.P., Hansen T.F. 1997. Phylogenies and the comparative method: a general approach to incorporating phylogenetic information into the analysis of interspecific data. Am. Nat. 149:646–667.
Nosil P. 2002. Transition rates between specialization and generalization in phytophagous insects. Evolution 56:1701–1706.
O'Meara B.C. 2012. Evolutionary inferences from phylogenies: a review of methods. Annu. Rev. Ecol. Evol. Syst. 43:267–285.
O'Meara B.C., An C., Sanderson M.J., Wainwright P.C. 2006. Testing for different rates of continuous trait evolution using likelihood. Evolution 60:922–933.
Paradis E., Claude J., Strimmer K. 2004. Ape: analyses of phylogenetics and evolution in R language. Bioinformatics 20:289–290.
Philippi T. 1993. Bet-hedging germination of desert annuals: beyond the first year. Am. Nat. 142:474–487.
Pianka E.R. 1974. Niche overlap and diffuse competition. Proc. Natl Acad. Sci. USA 71:2141–2145.
Rambaut A., Drummond A. 2007. Tracer v1.4. Available from: URL http://beast.bio.ed.ac.uk/tracer.
Ree R.H., Moore B.R., Webb C.O., Donoghue M.J. 2005. A likelihood framework for inferring the evolution of geographic range on phylogenetic trees. Evolution 59:2299–2311.
Ree R.H., Smith S.A. 2008. Maximum likelihood inference of geographic range evolution by dispersal, local extinction, and cladogenesis. Syst. Biol. 57:4–14.
Reveal J.L. 1989. The eriogonoid flora of California (Polygonaceae: Eriogonoideae). Phytologia 66:295–414.
Revell L.J. 2009. Size-correction and principal components for interspecific comparative studies. Evolution 63:3258–3268.
Revell L.J. 2012. Phytools: an R package for phylogenetic comparative biology (and other things). Method. Ecol. Evol. 3:217–223.
Revell L.J., Harmon L.J., Collar D.C. 2008. Phylogenetic signal, evolutionary process, and rate. Syst. Biol. 57:591–601.
Revell L.J., Reynolds G.R. 2012. A new Bayesian method for fitting evolutionary models to comparative data with intraspecific variation. Evolution 66:2697–2707.
Rohlf F.J. 2001. Comparative methods for the analysis of continuous variables: geometric interpretations. Evolution 2143–2160.
Ronquist F., Huelsenbeck J.P. 2003. Mrbayes 3: Bayesian phylogenetic inference under mixed models. Bioinformatics 19:1572–1574.
Ronquist F., Teslenko M., van der Mark P., Ayres D.L., Darling A., Höhna S., Larget B., Liu L., Suchard M.A., Huelsenbeck J.P. 2012. MrBayes 3.2: efficient Bayesian phylogenetic inference and model choice across a large model space. Syst. Biol. 61: 539–542.
Roughgarden J. 1972. Evolution of niche width. Am. Nat. 106:683–718.
Roughgarden J. 1983. Competition and theory in community ecology. Am. Nat. 122:583–601.
Salamin N., Wüest R.O., Lavergne S., Thuiller W., Pearman P.B. 2010. Assessing rapid evolution in a changing environment. Trends Ecol. Evol. 25:692–698.
Sanchez A., Kron K.A. 2008. Phylogenetics of Polygonaceae with an emphasis on the evolution of Eriogonoideae. Syst. Bot. 33:87–96.
Schluter D. 2000. The ecology of adaptive radiation. Oxford: Oxford University Press.
Silvestro D., Kostikova A., Litsios G., Pearman P.B., Salamin N. 2015. Measurement errors should always be incorporated in phylogenetic comparative analysis. Method. Ecol. Evol. 6:340–346.
Slater G.J., Harmon L.J., Alfaro M.E. 2012. Integrating fossils with molecular phylogenies improves inference of trait evolution. Evolution 66:3931–3944.
Stebbins G.L., Major J. 1965. Endemism and speciation in the California flora. Ecol. Monogr. 35:1–35.
Turelli M. 1984. Heritable genetic variation via mutation-selection balance: Lerch's zeta meets the abdominal bristle. Theor. Popul. Biol. 25:138–193.
Turelli M. 1985. Effects of pleiotropy on predictions concerning mutation-selection balance for polygenic traits. Genetics 165–195.
Turelli M., Gillespie J.H., Lande R. 1988. Rate tests for selection on quantitative characters during macroevolution and microevolution. Evolution 42:1085–1089.
Urbanski J., Mogi M., ODonnell D., DeCotiis M., Toma T., Armbruster P. 2012. Rapid adaptive evolution of photoperiodic response during invasion and range expansion across a climatic gradient. Am. Nat. 179:490–500.
Uyeda J.C., Harmon L. 2014. A novel bayesian method for inferring and interpreting the dynamics of adaptive landscapes from phylogenetic comparative data. Syst. Biol. 63:902–918.
Violle C., Enquist B.J., McGill B.J., Jiang L., Albert C.H., Hulshof C., Jung V., Messier J. 2012. The return of the variance: intraspecific variability in community ecology. Trends Ecol. Evol. 27:244–252.
Whitlock M.C. 1996. The red queen beats the jack-of-all-trades: the limitations on the evolution of phenotypic plasticity and niche breadth. Am. Nat. 148:S65–S77.
Whittaker R.H. 1960. Vegetation of the Siskiyou mountains, Oregon and California. Ecol. Monogr. 30:279–338.
Xie W., Lewis P.O., Fan Y., Kuo L., Chen M.-H. 2011. Improving marginal likelihood estimation for bayesian phylogenetic model selection. Syst. Biol. 60:150–160.

Downloaded from https://academic.oup.com/sysbio/article-abstract/65/3/417/2468958 by UB Leipzig user on 25 October 2019